# Metals in PET/CT: Causes And Reduction of Artifacts in PET Images

Catherine Lemmens and Johan Nuyts

***Abstract*— Metallic objects create artifacts in the PET/CT images. In this work, it is investigated which are the causes of the metal artifacts in the PET images and how these artifacts can be reduced. Based on a simulation study and some phantom measurements, it was found that the main cause for artifacts is an over-and underestimation of the PET attenuation values. Secondly movement also plays an important role in the creation of the PET metal artifacts. To reduce the metal artifacts two methods were proposed: 1) a modified conversion method which ensures the assignment of more correct PET attenuation to the metals, and 2) a simple registration procedure to reduce the motion-related metal artifacts. Both methods are successful in reducing the metal artifacts in the PET images.**

## I. Introduction

During the last decade, positron emission tomography (PET) in combination with computed tomography (CT) has worked his way into the daily clinical practice. PET/CT is used for diagnosis, staging and follow-up in oncology [1]. But also in other areas, such as neurology and treatment planning, the importance of PET/CT is steadily growing [1], [2]. Compared to the traditional standalone PET system, the use of a CT-based attenuation correction resulted in a reduction of the examination time, increasing patients comfort and clinical throughput. In addition to this, the CT images are almost noise-free compared to images obtained with the traditional transmission scans. However, the use of CT images for the attenuation correction of the PET gave also rise to some new challenges [1]. Firstly, there can be a mismatch between CT and PET due to voluntary patient motion, respiration, cardiac motion and bowel movement. Secondly, the conversion of CT images to PET attenuation maps assumes each material is a mixture of either air and water or of water and bone. However, the contrast media used in CT and metallic objects do not fulfill this assumption. Both problems can result in artifacts in the PET images.

In this paper the focus will be on the artifacts related to the presence of metallic objects like hip protheses and dental fillings in the patient. In the literature several papers have discussed metal artifacts in PET/CT. Goerres and co-workers [3], [4], [5], [6] found that the most common metal-related artifact is a false increase in tracer concentration adjacent to the metal. They also stated that shape and density of the metal are important for the presence and the severity of the artifacts and that movement of the metallic object increases the artifacts. In [7] it was stated that high-density materials do not show a false increased uptake without motion. The studies [8] and [9] investigated whether pacemakers, pacemaker leads and implantable cardioverter defibrillator (ICD) leads give rise to artifacts. Again the conclusion was that the artifacts are dependent on the density of the metal. The dense ICD leads sometimes gave rise to artifacts whereas with the less dense pacemaker leads no artifacts were seen. The very thin deep brain stimulation leads in [10] didn't produce any artifacts in the brain. In [11] the presence of EEG electrodes resulted in hot-spot artifacts at the location of the electrodes but no visual differences were seen inside the brain.

In order to reduce the metal artifacts in the PET images some methods were proposed. In [12] a segmentation of the CT image was applied such that all metal pixels received the attenuation value of water. In this way, artifacts disappeared and the resulting attenuation corrected PET images were similar to those obtained with a traditional transmission source. In the approach of [13], metal pixels again received the attenuation value of water. In [14] a metal artifact reduction (MAR) algorithm was applied to the CT images which resulted in the reduction of the metal artifacts both in CT and PET images. This is in contrast to a recent study of patients with dental implants [15] where it was found that although the application of a MAR algorithm [16] to the CT images resulted in less artifacts, there were no noticeable differences between the original and the MAR-corrected PET images. In [17] an algorithm was developed to reduce the artifacts in the CT-based attenuation maps. It was shown that the use of an erroneous attenuation map can result in false positive and false negative lesions.

In the first part of this paper the incidence and the appearance of metal artifacts in PET images is investigated and the results obtained are checked with the current literature. The effectiveness of the algorithms, discussed above, to reduce the metal artifacts in PET images is studied. In the second part, two methods to reduce the PET metal artifacts are proposed based on the results obtained in the first part: (1) a modified conversion method and (2) a method to reduce the metal artifacts due to movement.

## II. Simulation and phantom measurements

In this part, the dependence of metal artifacts in PET on size, density, shape and movement of the metal is investigated. The effectiveness of two methods, described in the literature, to reduce the metal artifacts in the PET images is also

The authors are with the Dept. of Nuclear Medicine, K.U.Leuven, Leuven, Belgium, (e-mail: catherine.lemmens@uz.kuleuven.be and johan.nuyts@uz.kuleuven.be). This work was supported by the "Institute for the Promotion of Innovation through Science and Technology in Flanders (IWT-Vlaanderen)".

investigated. For this purpose, PET/CT data were simulated and several phantom measurements were performed.

### A. Simulations

For the simulation of CT data, the 2D-fanbeam simulator described in [18] was used. This simulation software takes into account the finite size of the focus and the detector elements, the energy spectrum and the blurring due to rotation. For the simulation of the PET data, scatters and randoms were neglected.

PET/CT data of an elliptical water phantom (30 $\times$ 20 cm) with a circular metal insert ($\phi$ = 2 cm) were simulated. Different types of metal were considered: aluminum, titanium, iron and silver. In this way the dependence of the artifacts on the density of the metal could be investigated.

To determine the importance of a movement in between the CT and PET data, the same phantom described above was considered but the metal in the CT data was moved by 5 mm with respect to the PET data. Two movements were considered, one in the horizontal direction (towards the center of the field of view (FOV)) and one in the vertical direction.

To be able to investigate the dependence on size and shape, two more phantoms were simulated. For the first phantom a circular water phantom ($\phi$ = 20 cm) with an electroencephalogram (EEG) electrode placed in the center was considered. This EEG electrode is very small ($\phi$ = 1 cm) and thin (1 mm). Two PET/CT datasets were obtained: one for a golden electrode and one for an electrode made out of titanium. For the second phantom, a simplistic head-shaped phantom (ellipse 20 $\times$ 14 cm) with two amalgam dental fillings ($\phi$ = 3 mm) in a set of teeth was simulated.

For all simulations described above, a uniform tracer distribution was assumed in the water part of the phantom and no activity was assumed in the metal. In addition, we also wanted to investigate the appearance of possible metal artifacts in the presence of a positive uptake around the metal. For this purpose an elliptical water phantom (30 $\times$ 20 cm) with two circular inserts ($\phi$ = 2 cm) surrounded with positive "lesions" was simulated. One insert was made of iron, the other was water-equivalent and served as a reference. The uptake around the inserts was three times higher than the background.

### B. Phantom measurements

The phantom measurements were acquired on the Biograph16 (Siemens Medical Solutions, Knoxville, TN) PET/CT scanner. The CT data were acquired at 120 kVp and 170 mAs with a slice thickness of 3 mm, using a 18 mm table feed per rotation and a rotation time of 0.5 s.

Several metal objects were placed in containers filled with $^{18}$F-FDG homogenously distributed throughout water. The objects considered were a hip prosthesis made out of steel, a port-a-cath made out of titanium, a silver electrode, a cylinder ($\phi$ = 3 cm, $h$ = 1 cm) made out of aluminum, a cylinder ($\phi$ = 2 cm, $h$ = 2 cm) made out of stainless steel, an iron cylinder ($\phi$ = 1 cm, $h$ = 1 cm), a dental filling (amalgam $\phi$ = 5 mm) enclosed in a small plastic cylinder and a piece of lead. Note that most of these objects were placed solely in a container and that in the case of multiple objects in one container, the objects were in different transaxial planes.

### C. PET/CT reconstruction procedure

In clinical practice, CT images are reconstructed with analytical algorithms [19] since the use of iterative reconstruction is still time-consuming. Usually the CT images are reconstructed using 512 $\times$ 512 pixels in the transaxial FOV. The CT number takes a value in between -1024 Hounsfield Units (HU) and 3071 HU unless one makes use of the extended CT scale [20]. In this case, the CT numbers are scaled down by a factor of 10 so that the CT number takes a value in between -10240 HU and 30710 HU in steps of 10 HU. Most metals have a CT number higher than 3071 HU so in the presence of metals, the use of the extended CT-scale may be beneficial [21].

In this paper, the 3D conebeam data were rebinned into a 2D parallel beam configuration. This allowed for the use of filtered back projection (FBP) for the reconstruction of the CT images. It was verified that these reconstructions were similar to the clinical ones. For the simulations, the 2D fanbeam data were also rebinned into a 2D parallel beam configuration to ensure similarity with the phantom data. All CT images are displayed with a 1000 HU window centered at 0 HU unless stated differently.

After CT reconstruction, the CT images need to be converted to a PET attenuation map. Current conversion methods assume that each material is either a mixture of air and water, or of water and bone [22], [23]. This assumption is quite good for all human tissues. However, it is not valid for most metals and for the contrast media used in CT imaging. This means that if the extended CT scale is used, the PET attenuation value of most metals will be overestimated, whereas if a maximum CT number of 3071 HU is applied, the PET attenuation of most metals may be underestimated. For the conversion into PET attenuation maps, the CT images are first downsampled to PET resolution, smoothed with 7 mm FWHM and then the conversion method is applied.

Today, most PET systems perform data acquisition in 3D. Before reconstruction the 3D PET sinograms are corrected for detector sensitivity, dead time, random coincidences, scatter [24] and attenuation, and converted to 2D sinograms using Fourier rebinning [25]. For reconstruction of the PET images corrected for attenuation, the sinograms are "uncorrected" for attenuation, and reconstructed with Attenuation Weighted Ordered Subset Expectation Maximization (AWOSEM) [26]. PET images not corrected for attenuation (PET-NO-AC) are also reconstructed using Maximum-Likelihood Expectation Maximization (MLEM), accelerated using a gradually decreasing number of subsets [27]. PET images are reconstructed using 336 $\times$ 336 pixels in the transaxial FOV. In the presence of metals, the literature states that it is recommended to also read the PET-NO-AC images in order to exclude false positive tracer uptake due to metal artifacts [3], [4] and [8].

For the attenuation correction of the PET images of the simulations several procedures will be used. The first one is the procedure used in clinical practice. This means a maximum

of 3071 HU is applied to the CT images reconstructed with FBP (CT-FBP). The corresponding PET images will simply be denoted by PET H FBP. In the second case, the extended CT scale will be used. These PET reconstructions will be denoted by PET Ext FBP. To investigate the effectiveness of two methods described in the literature to reduce the artifacts in the PET images, three more PET reconstruction procedures were considered. As stated in the introduction, the use of a MAR algorithm for CT could also reduce the PET metal artifacts. Therefore, instead of using the artifactual CT-FBP images, the reference artifact-free CT images (CT-REF) will be used for the attenuation correction of the PET in the simulations (which corresponds to ideal artifact suppression). As in clinical practice, a maximum of 3071 HU will also be applied here. These PET reconstructions will be denoted by PET H REF. Instead of applying the maximum CT number, the combination of the extended CT scale with the artifact-free CT image was also considered. The corresponding PET images will be denoted by PET Ext REF. For the last procedure, the metal pixels in the CT-FBP images will be replaced by water pixels. The resulting PET reconstructions are denoted by PET W FBP. These last procedures are expected to produce less artifacts in the PET images.

### *D. Results and Discussion*

*1) Simulations:* Figure 1 shows the results of the simulations. From the first four rows, one can see that an increase in metal density results in an increase of the starbust-artifact and the noise in the CT images. The higher the density, the bigger the cold spot area in and around the metal will be, both in PET-NO-AC and PET H FBP images. For aluminum no extension of the cold area was seen. This is because aluminum has a CT number below 3071 HU and with current conversion methods, the obtained PET attenuation is more or less correct. When the extended CT scale is used, a hot spot artifact surrounding the metal appears in the PET Ext FBP images. The tracer concentration around the metal increases with increasing density which is logical since the overestimation of the PET attenuation is increasing in the same time. When the CT-REF image is used for the attenuation correction of the PET, the PET H REF image is suffering from small hot spots in the direction of the highest attenuation as the density of the metal increases. The replacement of the metal pixels with water pixels gives no hot spots (PET W FBP). However, when comparing with the conventional PET H FBP images, the use of this method results in an even bigger expansion of the cold spot area. If one uses the artifact-free CT image in combination with the extended CT-scale, the PET Ext REF images suffer from a hot spot artifact covering the entire metal. Again, the intensity of the hot spot increases with increasing density of the metal.

It is rather surprising that the use of an artifact-free CT image gives rise to hot spot artifacts in the PET images (PET H REF) whereas the PET image corrected with the artifactual CT image (PET H FBP) doesn't suffer from these artifacts. We believe this can be explained by the following. In the direction of the lowest attenuation (here vertical direction), higher amounts of activity are measured, so the reconstruction algorithm will "trust" those data more than the ones in the direction of highest attenuation (horizontal direction). Since the reconstruction algorithm relies more on the vertical data and since the attenuation value of the metal is underestimated with the current conversion methods, the reconstruction algorithm will assign less activity than the truth in the direction the highest activity was measured. However, now the reconstruction algorithm has problems to explain the data in the oblique lines, since there the reconstruction has less activity than measured. Since the reconstruction algorithm still relies more on the oblique lines than on the horizontal lines (lowest activity measurement), it will create hot spots in the direction of lowest activity measurement. This explains why an extension of the cold area is observed in combination with hot spots in the PET H REF images. In the case where the artifactual CT-FBP image is used for attenuation correction no hot spots are seen. In the presence of artifacts, the attenuation in the direction of lowest total attenuation (vertical direction) will increase -compared to the artifact-free images- due to the high intensity artifacts. This implies that the extension of the cold area will decrease since the attenuation correction factors (ACF) are more correct in that direction. Right next to the metal, in the lowest attenuation direction, and in the oblique direction, the ACF are underestimated (in the CT-reference case they were correct) due to the low intensity artifacts. This in combination with the reconstruction of an extended cold area will ensure that the estimated measurement based on the reconstruction will agree with the measured data, so that no hot spot artifacts are created in the direction of lowest activity measurement.

In the case where the extended CT scale is used, there is also a difference between the PET images corrected for attenuation with the artifactual CT-FBP image and with the CT-REF image. In the artifactual CT-FBP images the metals suffer from cupping. This means the CT number of the metal is depressed towards the center of the metal. Therefore the PET attenuation values in the center of the metal will be closer to their real values so that no hot spot is created inside the metal. At the edge of the metal, PET attenuation is overestimated resulting in a hot spot surrounding the metal.

Based on these first simulations, one could conclude that the PET images reconstructed with the current clinical procedure (PET H FBP) are the images with the least artifacts. It follows from this that the use of any the artifact-reducing algorithms seems not beneficial.

In the fifth row of fig. 1, the results of the horizontal movement in between CT and PET are shown in the case of the iron insert. As can be seen, all PET reconstructions, except for PET W FBP, suffer from hot spot artifacts in the direction the CT was moved. At the location of these hot spots, the PET attenuation values are overestimated, so the replacement of the metal pixels with water will eliminate the hot spot artifact as can be seen in PET W FBP. However, an extended cold spot area around the metal is still present in PET W FBP. Therefore one can conclude that replacing metal by water is a simple solution to suppress the hot spot artifacts in the case movement has occurred.

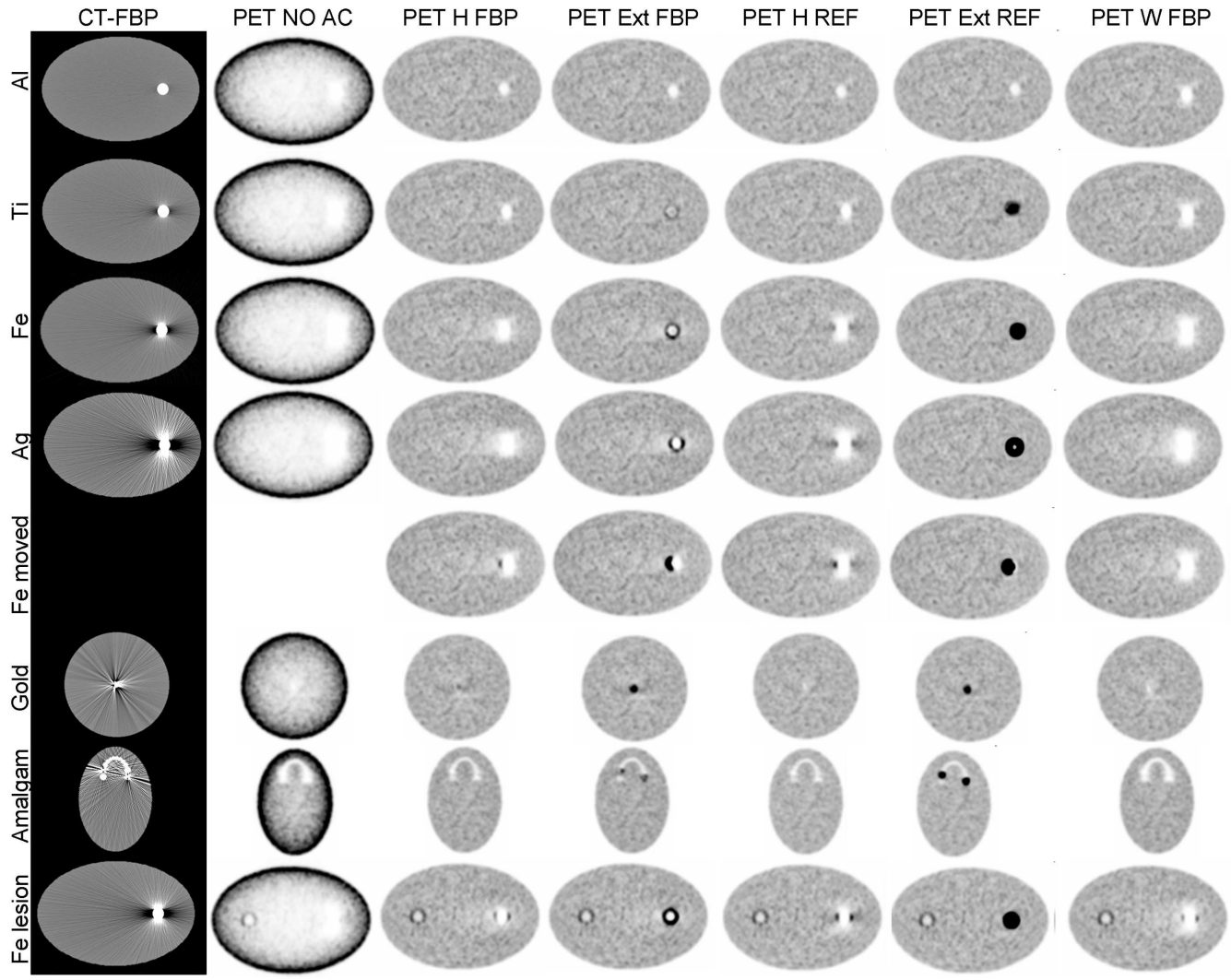


Fig. 1. The results of the simulations. Each row represents a different metallic object. From left to right: The CT image reconstructed with FBP, the PET-NO-AC image, the PET H FBP image, the PET image using CT-FBP for AC and the extended CT-scale (PET Ext FBP), the PET image when the artifact-free CT image was used for attenuation (PET H REF), the PET image using the artifact-free CT image for AC and the extended CT-scale (PET Ext REF), and the PET image when the metal pixels in the CT-FBP image were replaced with water (PET W FBP).

When the movement occurs in the vertical direction, no hot spot artifact is created in the PET H FBP image but the appearance of the cold spot area is slightly modified (image not shown). A large movement ($\approx$ cm) in the vertical direction will give rise to hot spot artifacts.

In the next simulations, an EEG electrode is considered. In the case of an electrode made out of titanium, the CT and PET images don't show any artifacts, moreover the electrode isn't visible in the PET reconstructions (images not shown). The results of the golden electrode are shown in the sixth row of fig. 1. In the CT-FBP image, the small electrode shows up as a "blob". This blob creates an overestimation of the ACF with the consequence that there is a hot spot artifact in the PET H FBP reconstruction [11]. The use of MAR algorithms are beneficial in this case since both PET H REF and PET W FBP do not suffer from hot spot artifacts. In the latter reconstructions one can even see a small cold spot at the location of the electrode.

The results of the head-shaped phantom with two dental fillings (last but one row in fig. 1) show no hot spot artifacts except for when the extended CT-scale is used (PET Ext FBP and PET Ext REF). This result is in agreement with the results of the patient study described in [15] where for patients with dental fillings no visual differences were seen between PET images corrected for attenuation with a CT-FBP image and a CT-image corrected for metal artifacts.

In the last row of fig. 1 the reconstructions in the presence of an increased uptake surrounding the metal are shown. When comparing to the reference uptake at the left of the phantom, one can see that the uptake around the metal is minimal in the PET H FBP image. If one now applies the guideline to compare with the PET-NO-AC image, one would designate the uptake around the metal as artifacts since there is no uptake visible in PET-NO-AC. This means one would miss a lesion. In PET H REF and PET W FBP the circle of uptake is also reduced to two hot spots whereas with PET Ext FBP and PET

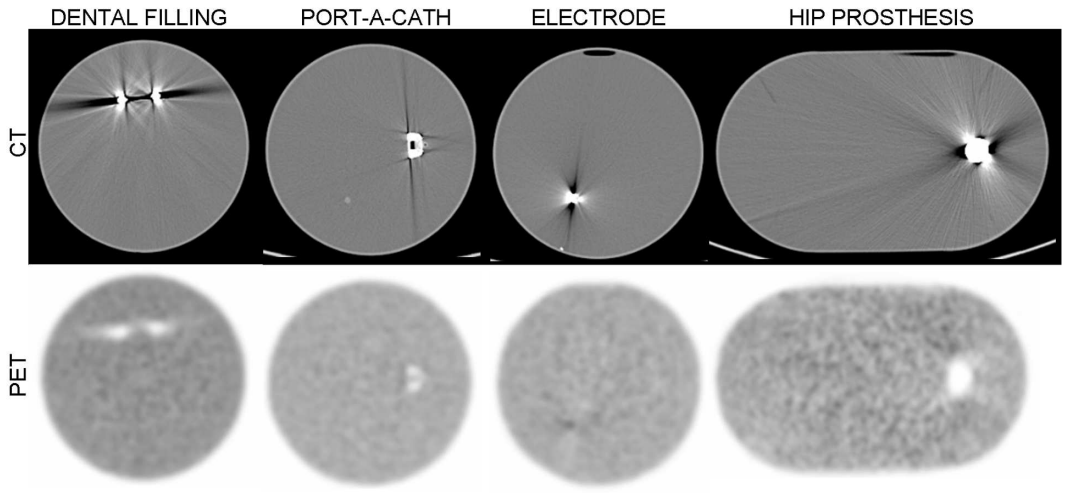


Fig. 2. Results of the phantom measurements. The top row shows the CT-FBP reconstructions. The bottom row shows the PET H FBP reconstructions.

Ext REF the uptake is clearly visible but too intense compared to the reference. In a similar experiment with a smaller insert ($\phi$ = 1 cm instead of 2 cm), the activity surrounding the insert did even not show at all in the PET H FBP and PET-NO-AC images, although the reference lesion was clearly visible (images not shown).

In this paper, we only considered iterative PET reconstructions. However, when PET reconstruction is done analytically using FBP, the appearance of the artifacts will change. In this latter case, the artifacts in the CT images will be ”burned” into the PET images: an increased CT number in the CT-FBP image will result in a hot spot artifact in the PET images, whereas a decreased CT-number will result in cold spot artifacts.

*2) Phantom measurements:* Most of the measured metal objects don’t show any hot spot artifacts in the PET images. The objects that cause hot spot artifacts are the silver electrode, as expected from the simulations, and the piece of lead. In fig. 2 transaxial slices of the clinical CT and PET reconstructions are shown for the dental fillings, the port-a-cath, the electrode and the hip prosthesis. In the PET reconstruction of the hip prothesis one can clearly see the extension of the cold area which is in agreement with the results of the simulations.

### *E. Conclusion*

From the experiments above one can draw several conclusions. First, the appearance of the artifacts in the PET images, either hot spots or an extended cold area, is very dependent on the density of the metal. The more dense the metal is, the more severe the artifacts will be. Whether or not a hot spot artifact will arise in the PET image, is an interplay between shape, size and density with density being the main player. For the cases relevant in the clinical setting, no hot spot artifacts were observed. This is in contrast to the literature where the most common artifact described is a hot spot. Secondly, dependent on the amount and the direction, movement can result in hot spot artifacts. It was demonstrated that the replacement of the metal pixels by water results in a suppression of the hot spot artifact. A third conclusion is that a positive lesion around a metallic object might be classified as an artifact or that the lesion doesn’t show at all. A last important conclusion is that the use of the extended CT scale, the use of an artefact-free CT image or the replacement of metal pixels with water doesn’t improve the quality of the PET reconstructions. So both overestimation and underestimation of the PET attenuation values of metallic objects result in artifacts.

Based on these conclusions, we postulate that the main cause of the metal artifacts is the assignment of incorrect PET attenuation values to the metal pixels. Secondary, movement of the metallic object in between CT and PET acquisition is a big malefactor.

## III. Proposed Methods

Based on the results of the simulations and phantom measurements, a new conversion method is proposed which will result in more accurate PET attenuation values of the metallic objects. Secondly, a simple method to suppress the artifacts due to movement is proposed.

### *A. Metal conversion*

The proposed conversion method, which will be called the metal conversion method, is a mixture-based model like the conversion methods used in clinical practice. For CT numbers below 3071 HU, the metal conversion is equal to the current conversion method [23]. For convenience, the value of 3071 HU will be called the cutoff-value. For CT numbers beyond 3071 HU, the metal conversion method assumes each tissue or material is a mixture of the cutoff-value -titanium, titanium-iron or iron-copper. An extension to other mixtures of metals is possible.

When an accurate conversion is used, it seems beneficial to use a MAR algorithm to suppress the artifacts in the CT images in order to obtain proper CT numbers. A slightly modified version of the MAR algorithm described in [16] is used for this purpose. In short the algorithm consists of the

following steps: First an initial reconstruction of the CT data is done. Based on this initial reconstruction, an absolute intensity and a smoothing prior are defined so that a Maximum-A-Posteriori [28] reconstruction can be performed which results in an artifact-free constrained image. This constrained image is then the basis for an image based projection completion method.

Two modifications are made to the MAR algorithm. Firstly, the initial reconstruction is done with the iterative maximum-likelihood polychromatic algorithm for CT (IMPACT) [29]. This algorithm models the polychromatic nature of the X-ray tube and therefore reduces the beamhardening artifacts such as the cupping effect. By using IMPACT for the initial reconstruction instead of FBP or an iterative reconstruction for transmission tomography (MLTR) [28] the cupping artifact inside the metal is reduced so that CT numbers inside the metal are more correct. Secondly, in the final artifact-reduced image all metal pixels will be replaced by the metal pixels from the initial IMPACT reconstruction.

To demonstrate the effectiveness of the newly proposed metal conversion method, it will be applied to the simulated objects discussed in the first part of this paper. In addition, to show the need for a MAR algorithm for CT, the metal conversion was also applied to the standard FBP images making a comparison between CT-FBP based AC and CT-MAR based AC possible.

### *B. Registration of metals*

In order to eliminate the metal artifacts in the PET images caused by movement of the patient, a registration of the CT image with the PET-NO-AC image can be performed. However, registration based on mutual information between CT and PET-NO-AC images is very difficult due to the limited amount of information available in the PET-NO-AC images. Reconstructing the PET-NO-AC images with a MLEM algorithm that allows negative values in the reconstruction (NEG-ML [30]) improves image quality, see fig. 3. However, registration between CT and PET-NO-AC reconstructed with NEG-ML still gives unsatisfying results. Therefore the following approach was taken.

By using NEG-ML, it is possible to segment the metal in an accurate way compared to the standard MLEM reconstruction where the borders of the metal are not clearly visible. In the PET-NO-AC MEG-ML images the metal appears as a region with negative values. By applying a threshold of 0.8 $cm^{-1}$ in the CT images, and by applying a region growing technique in the PET-NO-AC NEG-ML images, two binary images of the metal are obtained. These binary images can then be registered rigidly by minimizing the sum of squared differences. Only a translational movement is allowed during registration. Afterwards the obtained transformation can be applied to the CT image in order to obtain registered metals.

To show the feasibility of the registration procedure, two patient studies were selected that showed a misregistration at the location of a metallic object. In the first patient, the object under consideration is a hip prosthesis, whereas in the second patient, movement of the teeth with dental fillings occurred. The reconstruction of the PET images was done using the newly proposed reconstruction procedure, so using MAR in combination with the metal conversion.

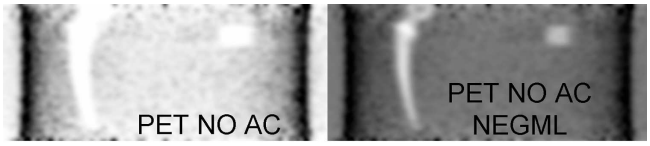


Fig. 3. Coronal slice through the PET-NO-AC and PET-NO-AC NEG-ML reconstruction of a phantom measurement with a hip prosthesis.

## IV. Results

### *A. Metal conversion*

The results of applying the metal conversion method to the CT-FBP and the CT-MAR images are shown in fig. 4. In the case of the titanium insert, the PET images corrected for attenuation with the CT-FBP images (PET M FBP) look similar to the PET images corrected for attenuation with the CT-MAR images (PET M MAR). Titanium isn't a very dense metal so the metal artifacts in the CT-FBP image are limited. On the other hand, with a more dense object like the iron insert, on sees that in the PET M FBP images the cold spot is spread out, whereas in the PET M MAR images, the cold spot is limited to the metallic object without any surrounding artifacts. So for these cases, the use of the metal conversion method in combination with the MAR algorithm is capable of eliminating the metal artifacts in the PET images.

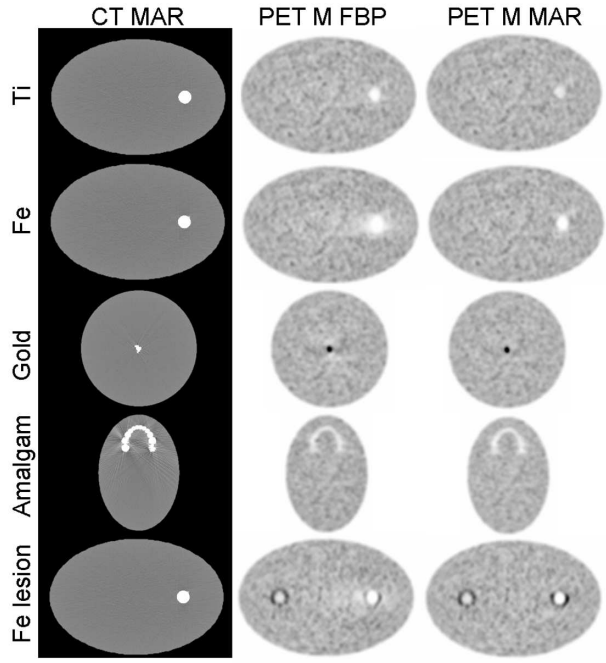


Fig. 4. Results of the simulations using the metal conversion.

In the simulation with the golden electrode, there is a hot spot in both PET M FBP and PET M MAR. The MAR algorithm isn't able to fully recover the shape of the small electrode so that it also shows up as a 'blob' in the CT-MAR images.

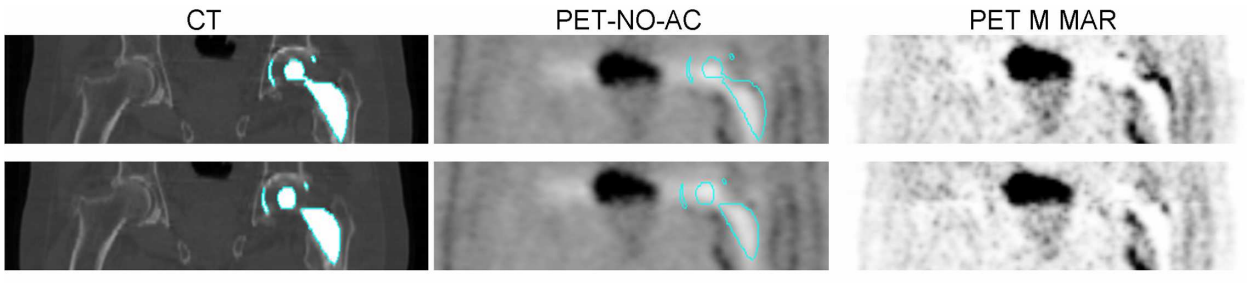


Fig. 5. Patient with movement of a hip prosthesis. The top row shows the CT MAR and PET images before registration. The bottom row shows the CT MAR and PET images obtained after registration. The contour of the metal object was defined in both cases on the CT image and transferred to the PET-NO-AC (NEG-ML) image to show mismatch/match. The maximum width (4096 HU) window was used to display the CT images.

In [11] the MAR algorithm was used in combination with the replacement of the metal pixels with a zero attenuation value in order to eliminate the hot spot artifacts due to the electrodes. So for the dense electrodes it seems that the use of a MAR algorithm in combination with the metal conversion method isn't beneficial. In the simulation of the amalgam dental fillings, the PET M FBP and the PET M MAR image look very similar except for a minuscule hot spot near the metal in PET M FBP. Already in the traditional approach no artifacts were seen, and the newly proposed procedure doesn't create any artifacts either.

In the presence of a lesion surrounding the metal object, the PET M FBP image shows some uptake around the metal but again, as was the case without the lesion, the cold region is spread out. In the PET M MAR image, the lesion is clearly visible although it seems to have a higher uptake when compared to the reference lesion at the left.

### *B. Registration of metals*

In the first patient, there is a misregistration between CT and PET as can be seen in the PET-NO-AC image of the top row of fig. 5. The misregistration results in a hot spot above the hip prosthesis (see the PET M MAR image). After applying the registration procedure, the hip prosthesis, delineated on the CT image, better fits the cold area of the PET-NO-AC image. If the PET is reconstructed again based on the registered CT image, the hot spot artifact has disappeared.

In the second patient, hot spot artifacts were present in the PET image due to a misregistration of the dental fillings (fig. 6). After applying the registration procedure, the hot spot artifacts are removed (bottom row fig. 5).

## V. Discussion

In this paper, we studied in which cases the presence of metallic objects gives rise to metal artifacts in the PET images in PET/CT and how these artifacts can be eliminated.

The appearance of the metal artifacts in the PET images (extended cold spot area or hot spot) is to a great extent determined by the density of the metal object. Higher density will result in bigger artifacts. Furthermore, the size of the metallic object and its shape also play an important role. For example, the golden electrode gave rise to a hot spot artifact in the PET H FBP images whereas a golden circle with the same diameter would result in an extended cold spot, as observed in another simulation experiment.

There are two main causes for metal artifacts in the PET images. The first one is the use of an incorrect PET attenuation value for the metal. In the clinical procedure, the current conversion method results in an underestimation of the PET attenuation values. The use of the extended CT-scale on the other hand will result in an overestimation of the metal giving rise to false positive tracer uptake. Therefore a new conversion method, called the metal conversion method, was proposed. The metal conversion method is a mixture based model which improves the assignment of PET attenuation values to the metallic objects. The use of the metal conversion implies that the CT number may not be limited to a value in between [-1024,3071] HU. Even the use of the extended CT-scale puts a limit to the CT number. In order to be able to apply the metal conversion to his full extent, CT images may not be saved into 12-bit images. A higher bit-number is needed to cover the full range of CT numbers of metallic objects.

Through simulations it was shown that by using the metal conversion method in combination with a MAR algorithm for CT reconstruction, the metal artifacts in the PET images could be reduced. The current evaluation was limited to visual analysis of a small set of simulations and measurements. A careful quantitative study is required to assess the bias associated with the proposed conversion method. We assume this bias will be small since for human tissues the conversion from CT to PET attenuation remains the same. In the presence of the dense EEG electrodes, the PET images reconstructed using the metal conversion and the MAR algorithm for CT didn't meet the expectations. This was due to the incapability of the MAR algorithm to completely eliminate the artifacts. So the search for good MAR algorithms must be continued.

With the current guideline to inspect the PET-NO-AC images to verify whether a positive tracer uptake in the PET images is a lesion (uptake visible in PET-NO-AC) or an artifact (no uptake visible in PET-NO-AC), lesions can be missed as was shown in the simulations. It would be optimal if diagnosis could be made based on one image namely the PET image.

The second cause for metal artifacts in the PET images is the movement of the metal in between acquisition of CT and PET. To eliminate these artifacts one can segment the metal out of the CT and PET-NO-AC NEG-ML image and then rigidly register those images. In order to obtain a good segmentation

of the metal in non-attenuation corrected PET images, the use of the NEG-ML algorithm for reconstruction is indispensable.

One could also use the NEG-ML algorithm for the reconstruction of the PET images. This will improve the visibility of the metal itself although it will not remove the artifacts related to the underestimation and overestimation of PET attenuation values. The same artifacts (cold spot extension and/or hot spots) would remain.

So in the presence of metallic objects, a possible procedure for reconstruction of the PET/CT images would be to firstly reconstruct the CT image using a MAR algorithm. Then the PET-NO-AC image can be reconstructed using NEG-ML. The CT and PET-NO-AC images should be checked for movement. In the case of movement, the CT image needs to be registered to the PET-NO-AC NEG-ML image. After alignment, the CT MAR image needs to be converted to PET attenuation values using the metal conversion. And finally the PET image can be reconstructed.

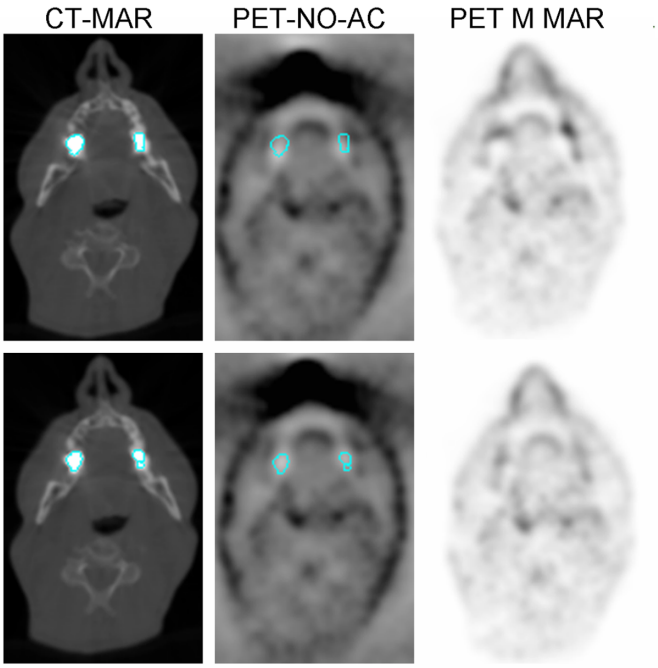


Fig. 6. Patient with movement of the head. The top row shows the CT MAR and PET images before registration. The bottom row shows the CT MAR and PET images obtained after registration. The contour of the metal object was defined in both cases on the CT image and transferred to the PET-NO-AC (NEG-ML) image to show mismach/match. The maximum width (4096 HU) window was used to display the CT images.

## VI. Acknowledgement

The authors thank David Faul, James Hamill and colleagues from Siemens for software and Karl Stierstorfer for help with the CT file format and information about the spectrum of the CT scanner. The authors thank Kathleen Vunckx for helpful advice.

## References

[1] D. W. Townsend, "Multimodality imaging of structure and function", *Phys med Biol*, vol. 53, R1-R39, 2008.

[2] H. Zaidi, M-L. Montadon and S. Meikle, "Strategies for attenuation compensation in neurological PET stusies", *NeuroImage*, vol. 34, 518-541, 2007.

[3] G. W. Goerres, T. F. Hany, E. Kamel et al., "Head and neck imaging with PET and PET/CT artefacts from dental metallic implants", *Eur J Nucl Med*, vol. 29, 367-370, 2002.

[4] G. W. Goerres, S. I. Ziegler, C. Burger et al., "Artifacts at PET and PET/CT cuased by metallic hip prosthetic material", *Radiology*, vol. 226, 577-584, 2003.

[5] G. W. Goerres, D. T. Schmid and G. K. Eyrich, "Do hardware artefacts influence the performance of head and neck PET scans in patients with oral cavity squamous cell cancer?", *Dentomaxillofac Radiol*, vol. 32, 365-371, 2003.

[6] E. M. Kamel, C. Burger, A. Buck et al., "Impact of metallic dental implants on CT-based attenuation correction in a combined PET/CT scanner", *Eur Radiol*, vol. 13, 724-728, 2003.

[7] T. Kaneta, K. Takanami, Y. Wakayama et al., "High-density materials do not always induce artifacts on PET/CT: what is responsible for the difference?", *Nucl Med Commun*, vol. 28, 495-499, 2007.

[8] B. S. Halpern, M. Dahlbom, C. Waldherr et al., "Cardiac pacemakers and central venous lines can induce focal artifacts on CT-corrected PET images", *J Nucl Med*, vol. 45, 290-293, 2004.

[9] F. P. DiFilippo and R. C. Brunken, "Do implanted pacemaker leads and ICD leads cause metal-related artifact in cardiac PET/CT?", *J Nucl Med*, vol. 46, 436-443, 2005.

[10] M. R. Ay and H. Zaidi, "Impact of X-ray tube settings and metallic leads on neurological PET imaging when using CT-based attenuation correction", *Nucl Instr Meth Phys Res A*, vol. 571, 411-414, 2007.

[11] C. Lemmens, M-L. Montandon, J. Nuyts et al., "Impact of metal artefacts due to EEG electrodes in brain PET/CT imaging", *Phys Med Biol*, vol. 53, 4417-4429, 2008.

[12] S. Mirzaei, M. Geurchaft, C. Bonnier et al., "Use of segmented CT transmission map to avoid metal artifacts in PET images by a PET-CT device", *BMC Nuclear Medicine*, vol. 5, 3, 2005.

[13] J. J. Hamill, R. C. Brunken, B. Bybel et al., "A knowledge-based method for reducing attenuation artefacts caused by cardiac appliances in myocardial PET/CT", *Phys Med Biol*, vol. 51, 2901-2918, 2006.

[14] K. P. Schäfers, R. Raupach and T. Beyer, "Combined $^{18}$F-FDG-PET/CT imaging of the head and neck", *Nuklearmedizin*, vol. 45, 219-222, 2006.

[15] C. Nahmias, C. Lemmens, D. Faul et al., "Does reducing CT artifacts from dental implants influence the PET interpretation in PET/CT studies of oral cancer and head and neck cancer?", *J Nucl Med*, vol. 49, 1047-1052, 2008.

[16] C. Lemmens, D. Faul and J. Nuyts, "Suppression of metal artiafcts in CT using a reconstruction procedure that combines MAP and projection completion", *Trans Med Imaging*, in press, 2008.

[17] J. A. Kennedy, O. Israel, A. Frenkel et al., "The reduction of artifacts due to metal hip implants in CT-attenuation corrected PET images from hybrid PET/CT scanners", *Med Bio Eng Comput*, vol. 45, 553-562, 2007.

[18] B. De Man, J. Nuyts, P. Dupont et al.,"Metal streak artifacts in X-ray computed tomography: a simulation study",*IEEE Trans Nucl Sci* vol. 46, 691-696, 1999.

[19] K. Stierstorfer, A. Rauscher, J. Boese et al., "Weighted FBP-a simple approximate 3D FBP algorithm for multislice spiral CT with good dose usage for arbritary pitch", *Phys Med Biol*, vol. 49, 2209-2218, 2004.

[20] C. Coolens and P. J. Childs, "Calibration of CT Hounsfield units for radiotherapy treatment planning of patients with metallic hip prostheses: the use of the extended CT-scale", *Phys Med Biol*, vol. 48, 1591-1603, 2003.

[21] T. M. Link, W. Berning, S. Scherf et al., "CT of metal implants: reduction of artifacts using an extended CT scale technique", *J Comput Assist Tomogr*, vol. 24, 165-172, 2000.

[22] P. E. Kinahan, D. W. Townsend, T. Beyer and D. Sashin, "Attenuation correction for a combined 3D PET/CT scanner", *Med Phys*, vol. 25 (10), 2046-2053, 1998.

[23] J. P. J. Carney, D. W. Townsend, V. Rappoport and B. Bendriem, "Method for transforming CT images for attenuation correction in PET/CT imaging", *Med Phys*, vol. 33 (4), 976-983, 2006.

[24] C. C. Watson, "New, faster, image-based scatter correction for 3D PET", *IEEE Trans. Nucl. Sci.*, vol. 47, 1587-1594, 2000.

[25] M. Defrise, P. E. Kinahan, D. W. Townsend et al., "Exact and approximate rebinning algorithms for 3-D PET data", *IEEE Trans Med Imaging*, vol. 16, 145-58, 1997.

[26] C. Comtat,P. E. Kinahan, M. Defrise et al., "Fast reconstruction of 3D PET data with accurate statistical modeling", *IEEE Trans Nucl Sci*, vol. 45 (3), 1083-1089, 1998.

[27] H. M. Hudson and R. S. Larkin, ”Accelerated image reconstruction using ordered subsets of projection data”, *IEEE Trans Med Imaging*, vol. 13, 601-609, 1994.
[28] B. De Man, J. Nuyts, P. Dupont et al., ”Reduction of metal streak artifacts in x-ray computed tomography using a transmission maximum a posteriori algorithm”, *IEEE Trans Nucl Sci*, vol. 47 (3), 977-981, 2000.
[29] B. De Man, J. Nuyts, P. Dupont et al.,”An iterative maximum-likelihood polychromatic algorithm for CT”, *IEEE Trans Med Imaging*, vol. 20 (10), 999-1008, 2001.
[30] J. Nuyts S. Stroobants, P. Dupont et al., ”Reducing loss of image quality because of the attenuation artifact in uncorrected PET whole-body images”, *J Nucl Med*, vol. 43 (8), 1054-1062, 2002.